PHYSICAL REVIEW B **67**, 180506(R) (2003)

# Spectroscopy of voltage dependence of oxygen movement in $YBa_2Cu_3O_{7-\delta}$

S. H. Huerth* and H. D. Hallen
*North Carolina State University, Raleigh, North Carolina 27695, USA*

B. Moeckly
*Conductus Inc., 969 W. Maude Avenue, Sunnyvale, California 94085-2802, USA*

(Received 31 March 2003; published 29 May 2003)

Injection of few-volt electrons at room temperature can displace oxygen atoms in the lattice of yttrium barium cuprate (YBCO). The metal cladding of a near-field scanning optical microscope (NSOM) probe tip is used as a tunnel electrode for locally injecting the electrons with controlled energies. The NSOM optical signal is used to detect changes in the local oxygen concentration. The data support bond breaking in a Franck-Condon-like effect causing enhanced diffusion of oxygen atoms in the lattice. The voltage dependence is consistent with the band structure of YBCO.

DOI: 10.1103/PhysRevB.67.180506 PACS number(s): 73.63.−b, 66.30.Qa, 68.37.Ef, 68.37.Uv

The movement of atoms induced by electron motion—electromigration or electron-induced motion (EIM)—has been studied in many systems.[1–6] There are a few possible processes by which EIM can occur. In the case of the classic electron-wind mechanism,[1,2,5,6] the atom motion is in the same direction as the current. We show here that this is not necessarily the case when few-eV electrons are used. In this case, a local electron interaction enhances the diffusion of an atom. Its motion is directed by the concentration gradient independent of the direction of electron injection. Naively, this localization of an electron interaction in a conductor seems unlikely, but it will occur when the electron can excite a carrier from a localized state on the atom rather than from the extended conduction states. The excitation places the atom in an unstable configuration, a Franck-Condon-like excitation, and the atom can move before relaxation if a vacancy is adjacent. Excitation from a localized state entails a threshold energy for the injected electron, which we measure for the case of oxygen motion in yttrium barium cuprate, $YBa_2Cu_3O_{7-d}$ (YBCO). It is interesting that the motion of oxygen described here shares many of the same qualitative features as the motion of vacancies in gold films with injection of few-eV tunnel electrons.[4,7–9] Both have *energy thresholds*, related to their respective band structures. Both exhibit atomic motion towards and away from the tunneling tip, underlining the diffusivity enhancement, not directed motion, of the effects. The EIM is limited to a single grain in both cases, indicating that *few-eV electrons are scattered strongly at grain boundaries* in quite disparate materials. There are differences, however. The topographies of the gold films change dramatically as the atoms move, whereas the oxygen atoms in YBCO move in a fixed lattice resulting in no detectable topographic change.[3] Only one component—the oxygen—in YBCO moves, whereas all the gold atoms are subject to displacement. This paper identifies the EIM mechanism and illustrates the properties noted above for YBCO, with detailed studies of the dosage (current×time) and spectroscopic (injected electron energy) dependence of oxygen motion.

The EIM of oxygen in YBCO results in changes in its superconducting properties, since they depend on the oxygen concentration.[10,11] The motion of the oxygen in YBCO is not surprising, since it is known to be mobile at elevated temperatures (450 °C), as used for annealing.[12] We have shown in prior studies that it can be induced to move rapidly at room temperature by classic electromigration[10] or electron-induced migration.[3,13] To better understand the mechanism of oxygen movement in YBCO while avoiding complications due to grain boundaries, we use a near-field scanning optical microscope (NSOM). The metal cladding of the NSOM probe provides a scanning tunneling microscope (STM) tip to pull (inject) electrons from (into) an industrial quality sample of YBCO. This induces movement of oxygen. We have shown that a reflection-mode near-field scanning optical microscope can be used to image oxygen concentration variations in YBCO.[3] Optical NSOM images taken before and after EIM are compared to eliminate the native background oxygen concentration variations and determine that oxygen has moved in the lattice and where the movement occurred.

The complete sample preparation description and a summary of the sample properties have been given.[3,14] The sample set included laser ablated thin films and reactively coevaporated thin films. Topographic scans of the laser ablated samples showed a grain size on the order of 250 nm versus a grain size of 200 nm for the coevaporated thin films. The samples were studied using a near-field scanning optical microscope as diagrammed in Fig. 1. Light from a Nanophase 532-nm, 1-ns, 6-mW, pulsed laser was coupled into an optical fiber terminated with an NSOM metal clad

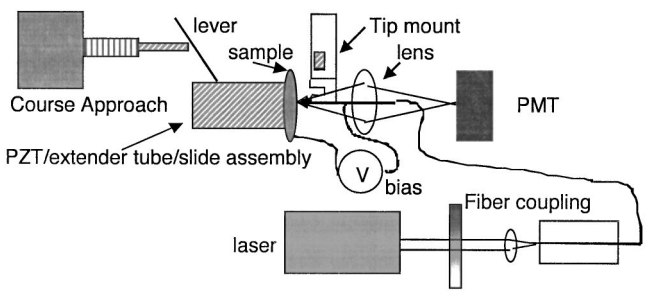


FIG. 1. Schematic of microscope setup.

 

probe. The probe illuminated the sample, and the reflected light was focused by an aspheric lens onto a photomultiplier tube (PMT). The output current of the PMT was preamplified with $10^6$ V/A, further amplified 100 times, and filtered to 10 Hz. The noise floor of the system corresponded to the signal from a sample with a reflectance of approximately $10^{-4}$. The NSOM instrument is similar to one described previously,[15] except that a stepper motor with a motion-reducing lever arm drives the coarse approach and a quartz crystal tuning fork[16] is used for topographic feedback. For EIM we used the following procedure:—the laser was turned off, the tip moved to the preselected location, feedback shut off and lateral feedback-dither shut off, a voltage applied to the sample, and the tip brought towards the sample until the desired tunnel current was measured on the metal clad probe. This state was maintained for the duration of the EIM, with slight manual adjustments to maintain the approximately constant (and recorded) tunnel current. The use of tunnel current feedback during the EIM was tried, but found not to be required for our thermally insulated, stable NSOM. Upon completion of the EIM, the probe was retracted from the surface and shear-force distance feedback reestablished. Variations in the surface oxygen concentration of YBCO, due to outdiffusion of oxygen from surface peaks in these *c*-axis normal films,[13] mask the changes induced by the electrons. To eliminate the initial oxygen variation effects, we take images before and after each EIM. The images are subtracted to form a difference image that shows the effects of EIM rather than the native oxygen variations. Since the EIM can take up to an hour, the microscope can drift. We correct for this by correlating the corresponding topographic images to determine shift and shifting the images before the subtraction.[17] We also scale (typically by a few percent) the images to correct for long-term laser drift and changes in optical probe throughput with wear.

To verify that the EIM does indeed result from electrons and not electric field, the laser illumination, or local heating, we performed several tests. Since the usual feedback distance in the NSOM is too far from the surface for a tunnel current, we can apply a voltage to the tip to create an electric field on the sample without any tunnel current. We used a relatively large voltage of $-3$ V for a total of 30 min. Before and after optical images showed no changes in the reflectivity implying no changes in the oxygen concentration. As usual, the topography was also unchanged. The effect of laser illumination was checked by examining the before, after, and difference images corresponding to laser illumination in one spot for 30 min. We saw no changes for either the red or green light. This result is expected to be wavelength dependent. The energy of the green light is 2.33 eV/photon, which is larger than the threshold energy measured from tunneling electrons, so one might expect an effect. The lack of a photon-induced excitation likely results from selection rules and lack of available energy levels. Effects due to local heating of the sample from either the laser light when scanning or from the tunnel electrons during the electron induced migration can be ruled out by an estimation of the temperature rise. Either source provides a few nanowatts of energy in a few-10's of nanometer (or deeper) cube. A relevant three-dimensional (3D) model for diffusion was given by La Rosa *et al.*[18] Symmetry was used to convert the local energy input at a surface to a spherically symmetric problem. The steady-state solution for the temperature rise at the origin, $\Delta T = 2Pr^2/k\Delta V$, can be evaluated for a conservative interaction volume $\Delta V = 1.25\times 10^{-22}$ m$^3$, input power $P = 3$ nW, thermal conductivity for YBCO, $k = 1.5$ W/Km, and radius $r = 50$ nm to find $\Delta T \sim 0.08°$. This should be compared to the 450 °C used to anneal oxygen in YBCO samples.[12] The induced local heating is negligible and is characteristic of the 3D diffusion applicable when the energy input is into a region much smaller than thermal length scales. The possibility of the effect being an electron-induced oxidation of the surface is unlikely since the region exposed to the tunneling electrons is more than two orders of magnitude smaller than the affected region.

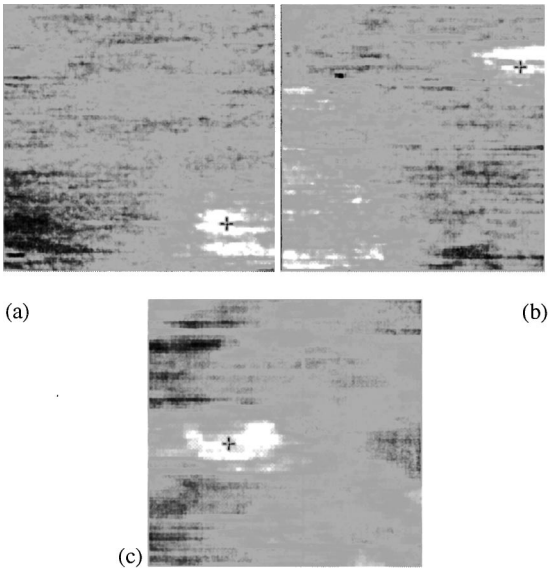


FIG. 2. Difference images for EIM at $-3$ V for 35 min at various tunnel currents. The crosshairs mark the area of oxygen concentration change. (a) 1200 nm square image, 0.4 a.u. gray range, tunnel current: 0.2 nA, percent contrast: 6%, effected spot size: 75 nm; (b) 1000 nm square image, 0.5 a.u. gray range, current: 0.5 nA, contrast: 19%, spot size: 100 nm; (c) 1500 nm square image, 0.7 a.u. gray range, current: 2.0 nA, contrast: 26%, spot size: 200 nm.

The dependence of EIM on electron dose (current $\times$ time) is shown in Fig. 2. This representative series of optical difference images (the after optical image minus the before optical image after taking into account drift) contains data taken with the same voltage ($-3$ V) and time (35 min), but with different tunnel currents (0.2, 0.5, 2 nA). The images show increasing spot size (effect) and increasing percent contrast. The whiter regions correspond to increasing reflectivity (for electric field normal to the surface) hence increased oxygen content[3,19] in the affected region. The medium gray over most of the images is zero or no oxygen change. Some fluctuations about this, of magnitude less than in the white-saturated EIM regions, are due to noise in the differencing process. Some of the larger black areas such as in (a) may represent real decrease in oxygenation. Percent contrast is used to quantify the effect and is defined to be the

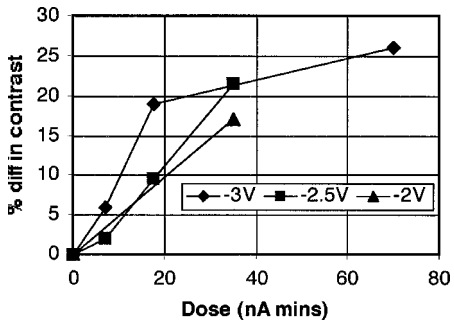


FIG. 3. Dose vs percent difference in contrast. As the voltage increases, the percent difference in contrast for the same dose increases. The limiting value at high dose is due to grain size or full oxygenation.

maximum optical signal minus the minimum optical signal divided by the average optical signal. This scaling removes the effects of long-term laser output drift and throughput variations with the probes used, allowing a quantitative comparison between different data sets. We have found data taken with different probes and samples still lie on the curves. The images show that the oxygen movement depends on the dose, and Fig. 3 illustrates that the dependence is linear for small doses for each voltage. The saturation behavior at larger doses results from other effects, primarily grain size,[3] saturation of oxygen sites, or leveling of the oxygen concentration within the grain volume.

The electron energy, or voltage, dependence is also evident in Fig. 3. The slope of the linear region for the three voltages shown on the graph increases with magnitude of the voltage. Not shown on the graph is data at $-1$ and 0 V, which resulted in no EIM for the coevaporated samples that were used for the data in this graph. The voltage threshold near $-1$ V for the effect is slightly sample dependent. Although multiple attempts at oxygen movement with $-1$ V on the coevaporated samples never produced an effect, we have seen a small effect at $-1$ V for samples grown by laser ablation. This may be due to disorder or defects that reduce the energy gaps in the laser-ablation-grown samples. The voltage dependence of the EIM slopes is shown in Fig. 4. It exhibits a threshold near $-1$ V followed by a rapid rise, a possible shoulder, and a continued increase for larger voltages. The error bars were calculated by estimating the error

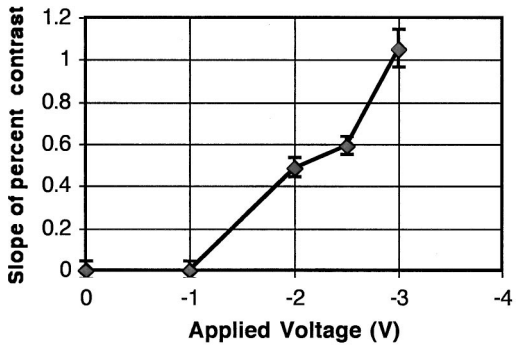


FIG. 4. Voltage dependence of EIM. The slope increases as the number of density of state increases.

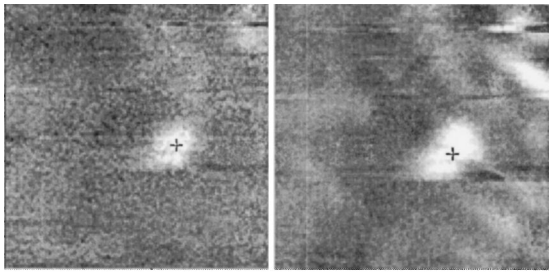

(a) (b)

FIG. 5. EIM with tunnel electron injection. Both images are 2500 nm square. A voltage bias of 3 V injecting a tunnel current of 1.4 nA for 34 min. The optical difference image is shown in (a) with a 1.2 a.u. gray range, and the optical image taken after the EIM is shown in (b) with 6.7–7.9 a.u. gray scale. The crosshairs mark the same position on both images.

of the percent contrast data, which is consistent with that expected from the linear fits to the data in Fig. 3, and evaluating the error of the least-squares fit slopes. The energy dependence can be explained in terms of the electron excitation spectra for YBCO evident in the band structure.[20] The essential feature is that it takes about 1 eV to excite an electron from a high density of states below the Fermi level to one above. The excitation is in a localized state so that it will not move from atom to atom before the atom has time to move. The hint of a shoulder in the voltage dependence is consistent with an energy range of lower density of states above $\sim$ 1 eV until a large number of bands become available at around 3 eV.

The picture of this process is somewhat complicated by the fact that, at negative voltages, we are pulling electrons towards the tip rather than injecting electrons into the YBCO. We can then think of excitation of the near-Fermi level electrons as an internal-Auger-like process. If the electron that drops to fill the state emptied by tunneling gives its energy to another electron at the Fermi level, as an Auger process, the broken bond can put the oxygen atom in an unstable potential, an antibonding state. When a neighboring oxygen is absent, this potential will be asymmetric as in a Franck-Condon-like excitation. If this broken bond is localized long enough for the oxygen to have time to move before the excitation moves or deexcites, then the electron will induce EIM in a manner similar to electron stimulated desorption.[21] A direct electron scattering process should also be capable of producing the excitation for EIM. We verify this with the use of a positive 3-V bias. The difference image is shown in Fig. 5(a) and shows a response that is easily seen even with the native oxygen variations in the ''after'' optical image, Fig. 5(b). Another interesting feature of this data is that the oxygen concentration is increased where the EIM took place, as it was for negative bias voltages. This underscores that the EIM process fundamentally increases the diffusivity of the oxygen, so that the oxygen atoms move into regions of lower oxygen content regardless of the direction of electron propagation. The surface tends to have a lower concentration due to outdiffusion, forcing oxygen to migrate

towards the surface and increasing the (z-polarized) reflectivity. The increased diffusivity is not due to a locally higher temperature, but to a nonequilibrium local electron energy promotion. The change in percent contrast of the data in Fig. 5 is similar, although slightly smaller than, the value expected for $-3$ V at the same dose. The reason why the effect is obvious in Fig. 5(b) is probably due to the fact that it, and not the others shown, was annealed at 450 °C for 30 min in a 90% oxygen, 10% nitrogen environment, which reduced the variation in surface oxygen content. The cross section for EIM will also depend upon the sign of the bias voltage.

In summary, measurements of the dose and voltage dependence of EIM in YBCO indicate that the bombardment by a few-eV electron increases the mobility of oxygen by breaking a bond or exciting a bonding electron into an antibonding state. If a neighboring oxygen atom is absent, the unstable potential for the oxygen will be asymmetric as in a Franck-Condon-like excitation. If the broken bond is localized on the single oxygen long enough for the oxygen to have time to move before the excitation moves or deexcites, then the electron will induce EIM. The likelihood of a neighboring vacancy on one side scales with concentration gradients, so the motion is enhanced diffusion. The energy dependence of the EIM is governed by the band structure of the material. The same type of process is expected to be active in many materials, as it depends on generic excitations from localized bands at the few-volt level. It will become increasingly important in nanoscale devices for which electrons may be injected across an interface with such energies, and its generic attributes are emphasized by similar grain boundary scattering and atom motion for the very different gold materials system.

*Current address: MCNC, Signal Electronics Division, 3021 Cornwallis Rd, Research Triangle Park, NC 27709.

[1] D. Young and A. Christou, IEEE Trans. Reliab. **43**, 186 (1994).
[2] J. R. Lloyd, Semicond. Sci. Technol. **12**, 1177 (1997).
[3] S. H. Huerth, M. P. Taylor, H. D. Hallen, and B. H. Moeckly, Appl. Phys. Lett. **77**, 2127 (2000).
[4] H. D. Hallen, A. Fernandez, T. Huang, R. A. Buhrman, and J. Silcox, Phys. Rev. Lett. **69**, 2931 (1992).
[5] A. Dasgupta and M. Pecht, IEEE Trans. Reliab. **40**, 531 (1991).
[6] J. R. Black, Reliability Physics **21**, 142 (1983).
[7] H. D. Hallen, A. Fernandez, T. Huang, R. A. Buhrman, and J. Silcox, J. Vac. Sci. Technol. B **9**, 585 (1991).
[8] H. D. Hallen, in *The Technology of Proximal Probe Lithography*, edited by C. Marrian (SPIE, Bellingham, 1993).
[9] H. D. Hallen and R. A. Buhrman, in *Atomic and Nanometer-Scale Modification of Materials: Fundamentals and Applications*, edited by P. Avouris (Kluwer, Dordrecht, 1993).
[10] B. H. Moeckly, D. K. Lathrop, and R. A. Buhrman, Phys. Rev. B **47**, 400 (1993).
[11] B. H. Moeckly, R. A. Buhrman, and P. E. Sulewski, Appl. Phys. Lett. **64**, 1427 (1994).
[12] E. Osquiguil, M. Maenhoudt, B. Wuyts, and Y. Bruynseraede, Appl. Phys. Lett. **60**, 1627 (1992).
[13] Suzanne Huerth, Michael Taylor, Michael Paesler, and Hans Hallen, in Proceedings of the Second Asia-Pacific Workshop on Near-field Optics, Beijing, China, 1999.
[14] B. Moeckly and K. Char, Physica C **265**, 283 (1996).
[15] C. L. Jahncke and H. D. Hallen, Rev. Sci. Instrum. **68**, 1759 (1997).
[16] Khaled Karrai and Robert D. Grober, Appl. Phys. Lett. **66**, 1842 (1995).
[17] S. H. Huerth and H. D. Hallen, J. Vac. Sci. Technol. B **21**, 714 (2003).
[18] A. H. LaRosa, C. L. Jahncke, and H. D. Hallen, Proc. SPIE **2384**, 101 (1995).
[19] J. Kircher *et al.*, Phys. Rev. B **44**, 217 (1991).
[20] W. Y. Ching, Y. Xu, G. L. Zhao, K. W. Wong, and F. Zandiehnadem, Phys. Rev. Lett. **59**, 1333 (1987).
[21] R. D. Ramsier and J. T. Yates Jr., Surf. Sci. Rep. **12**, 243 (1991).